# Power Factor Correction of Three-Phase PWM AC Chopper Fed Induction Motor Drive System Using HBCC Technique

**MOHAMED K. METWALY**[1,2], **HAITHAM Z. AZAZI**[2,3], **SAID A. DERAZ**[2,4], **MOHAMED E. DESSOUKI**[4,5], **AND MOHAMED S. ZAKY**[2,6]

[1]Electrical Engineering Department, Faculty of Engineering, Taif University, Taif 21974, Saudi Arabia
[2]Electrical Engineering Department, Faculty of Engineering, Menoufia University, Shibin El-Kom 32511, Egypt
[3]Department of Electrical Engineering, College of Engineering, King Khalid University, Abha 61421, Saudi Arabia
[4]Electrical Engineering Department, Faculty of Engineering, King Abdulaziz University, Rabigh 21911, Saudi Arabia
[5]Electrical Engineering Department, Faculty of Engineering, Port Said University, Port Said 42526, Egypt
[6]Department of Electrical Engineering, Northern Border University, Arar 1321, Saudi Arabia

Corresponding author: Mohamed K. Metwaly (mohkamel2007@yahoo.com)

**ABSTRACT** In this paper, a new control strategy for an induction motor (IM) drive system fed from three-phase pulse width modulation (PWM) ac chopper is proposed. The main objective of the proposed control scheme is to achieve input power factor correction (PFC) of the IM drive system under different operating conditions. PFC is achieved by continuously forcing the actual three-phase supply currents with the corresponding reference currents, which are generated in phase with the supply voltages, using hysteresis band current control (HBCC) technique. The proposed control strategy has two loops: the inner loop and outer loop. The output of the outer loop is the magnitude of the supply reference current resulting from either speed controller or startup controller, whereas the output of the inner loop is PWM signals of the ac chopper. The proposed ac chopper features a smaller number of active semiconductor switches, four IGBTs, with only two PWM gate signals. As a result, the proposed system is simple, reliable, highly efficient, and cost effective. Mathematical analysis of the drive system is presented. Components of the input *LC* filter are designed using frequency response. The IM drive system is modeled using MATLAB/SIMULINK, and a laboratory prototype was built and tested. The simulation and experimental results confirm the validity and robustness of the proposed control strategy.

**INDEX TERMS** Hysteresis band current control, induction motor drive, power factor correction, pulse width modulation, three-phase AC chopper.

## I. INTRODUCTION

AC voltage regulators, also called as AC voltage controllers, are used in various applications that require a regulated AC voltage. Lighting control using dimmer circuits, domestic and industrial heating, speed control and soft starters for the induction motors are examples of such applications [1], [2]. Different topologies with different control methods of these regulators in single phase applications and also in three phase applications are presented. The purpose of AC voltage controller is to vary the root mean square (RMS) value of its output that applied to the load circuit. There are

three control methods are offered to achieve this objective; ON/OFF method, phase angle (PA) method and pulse width modulation (PWM) method. All three control methods can be implemented in both single-phase and three-phase applications.

In ON/OFF control method, thyristors (i.e. silicon-controlled rectifiers) are used as power switches to connect/disconnect the circuit of the load to/from the AC voltage source continuously. Connection is occurred for a few integral cycles and disconnection for the next few cycles of the feeding voltage. Adjusting the number of conducted and interrupted cycles controls the RMS magnitude of the output voltage. In ON/OFF method, the generated harmonics by the switching actions are reduced as silicon-controlled
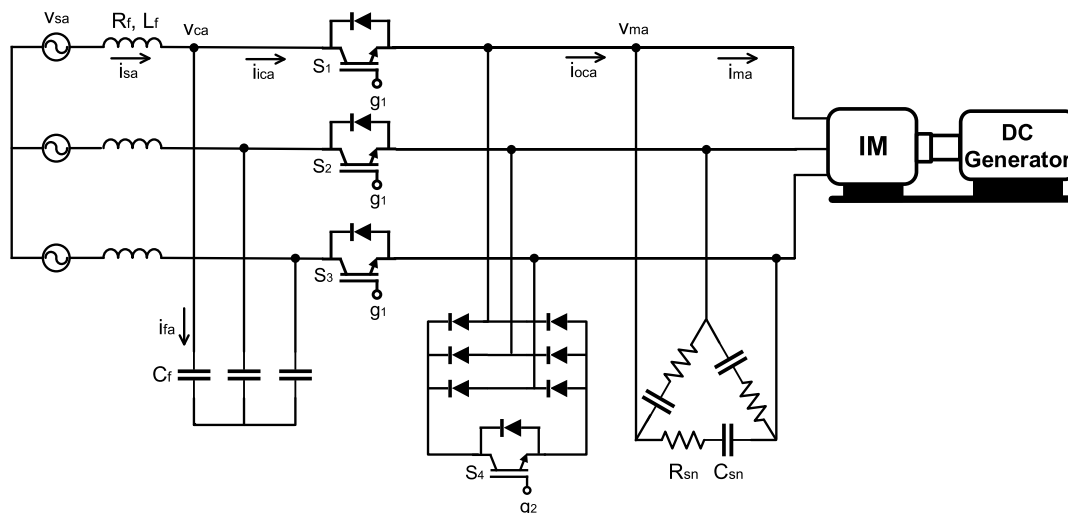
**FIGURE 1.** Power circuit of the proposed three-phase PWM AC chopper fed an IM drive system.

rectifiers (SCRs) are switched ON at zero voltage and switched OFF at zero current. However, undesirable sub-harmonic components may be produced [3]. Applications of this method are restricted to heating and temperature control systems due to the discontinuity of the power source at low demand levels.

In PA control method, the output of the AC voltage controller is regulated by adjusting the firing angles of SCRs. The power circuit of a single-phase regulator with PA control method is generally consisted of two thyristors which are joined back to back between the AC source and the load circuit, while three-phase regulator is composed of three pairs of SCRs. In [4], [5], soft starting for induction motor (IM) fed from a thyristorized voltage regulator is presented. The artificial techniques are utilized to adjust the motor voltage by varying the firing angles of the thyristors at certain operating instant of speed and torque commands. In [6], a voltage ramp technique is presented for starting of an AC motor. The voltage, in ramp technique, is increased gradually by adjusting the SCRs firing angles during starting of the motor. In [7], [8], a closed loop current control approach that determines the firing angles of thyristors required to keep the motor current at starting instant within a limit value is presented. In these approaches, a smooth start-up of the IM is obtained. However, numerous sensors and zero crossing detection (ZCD) circuits are required which make these controllers are complicated and expensive. In addition, the thyristorized AC voltage controller provides significant harmonics and low input power factor (PF) even if the load is a pure resistive. Recent developments in semiconductor switches make it possible to replace SCRs by modern power semiconductor switches like MOSFETs and IGBTs. Using PWM control method with the modern power switches, the AC voltage regulators performance can be enhanced in terms of harmonics, filter size, input PF and voltage control range [9]–[11]. In [12], a speed control of two-phase IM fed from single phase PWM

AC chopper is presented. The chopper has power circuit that consists of four IGBT switches. The RMS value of the motor voltage is controlled by changing the duty ratio of the chopper IGBTs and hence the motor speed is adjusted. This chopper is working in buck mode. Buck and boost modes are presented in [13]. Performance of single phase PWM AC chopper can be further improved using voltage harmonic elimination techniques. An approach using a genetic algorithm (GA) is presented in [14]. A phase shifting method for enhancing the input PF of a single phase PWM AC chopper is presented in [15], [16]. Phase shifting of the output voltage is achieved using asymmetrical pulse width modulation (APWM) as a control strategy. Performance comparison between conventional, symmetrical and asymmetrical PWM techniques is presented in [17]. However, phase shifting method decreases the control range of the chopper output voltage. Optimal values of the PWM single phase AC chopper parameters were selected to achieve a unity PF in [18]. An extinction angle control technique for PF improvement of a single-phase AC voltage controller fed an IM is presented in [19]. Different topologies of three phase PWM AC chopper in different applications are presented in [20]–[23]. A three phase PWM AC chopper, has eight IGBTs, feeds an IM is presented in [24]. A configuration of the three-phase chopper with six IGBTs for soft starting of three phase IM is presented in [25], while a four-IGBT configuration is presented in [26]. However, these configurations have low PF. A method of determining the operating PF of the three-phase IM using only the measured current and the manufacturer data of the motor is presented in [27]. In [28], a new asymmetrical pulse width modulated (APWM) controller for AC chopper fed three-phase IM drive is proposed. In [29], a hysteresis band current control (HBCC) approach is used to control the switching of the three-phase chopper fed three phase AC load. Using HBCC technique, balanced three phase sinusoidal currents are obtained. However, the power circuit of this system

uses six IGBTs with six gate pulses which make the system complex and expensive. Furthermore, the input PF of this approach is low.

Although researchers focused on PFC of single-phase PWM AC choppers, they have been given a little attention of PFC of three-phase choppers. PFC is important in order to comply with the necessaries of the international standards [30], [31]. On the other side, the reduction in the amount of semiconductor devices and introducing new control strategies are essential for control simplicity, reliability, higher efficiency and lower cost.

In this article, a new control strategy for PFC of three phase PWM AC chopper using HBCC technique fed three phase squirrel cage IM with soft starting and speed control operating modes is proposed. The power circuit of the proposed control strategy is simple, reliable, high efficiency and low cost as it has reduced number of power semiconductor switches. The three phase PWM AC chopper consists of four IGBTs. A new closed-loop control strategy, that uses only two gate pulses to drive the four IGBTs, is achieved. The proposed control strategy has three main control objectives: soft starting, speed control and input PFC, which are achieved by adjusting the RMS value of the input voltage fed the IM terminals. The proposed control strategy is investigated, analyzed and simulation results are obtained under different testing conditions. A laboratory prototype model is implemented based on the proposed control strategy. The experimental setup consists of a 1.5 hp squirrel cage IM coupled mechanically with a DC generator for loading purpose, a four-switch PWM AC chopper and a DSP DS-1104 control board. The experimental waveforms are obtained and compared with corresponding simulation waveforms. The rest of the article is organized as: first, description and operating modes of the proposed control strategy is discussed. Then, mathematical analysis of the proposed control strategy is introduced. Finally, the simulation and laboratory waveforms are collected and the article findings are concluded.

## II. SYSTEM DESCRIPTION AND OPERATION PRINCIPLE

Fig. 1 freewheeling stage, the power switch represents a schematic diagram of the proposed three phase PWM AC chopper fed an IM. The chopper is composed only of four power electronics switches ($S_1$, $S_2$, $S_3$ and $S_4$) that are illustrated in the figure. The three power switches ($S_1$, $S_2$ and $S_3$) are series-connected with the motor. While, the power switch ($S_4$) is parallel-connected via a poly phase bridge rectifier with the motor. The series-connected switches are utilized to continuously connect and disconnect the motor to and from the AC supply, respectively. Hence, they regulate the delivered power to the motor. While the parallel-connected switch ($S_4$) offers a freewheeling way for discharging the energy kept in the motor windings when the series-connected switches are turned OFF. As series and parallel devices operate in a complementary way, a dead time is introduced to avoid the commutation problems. There are three operating stages: active, freewheeling and dead time. In dead time period,
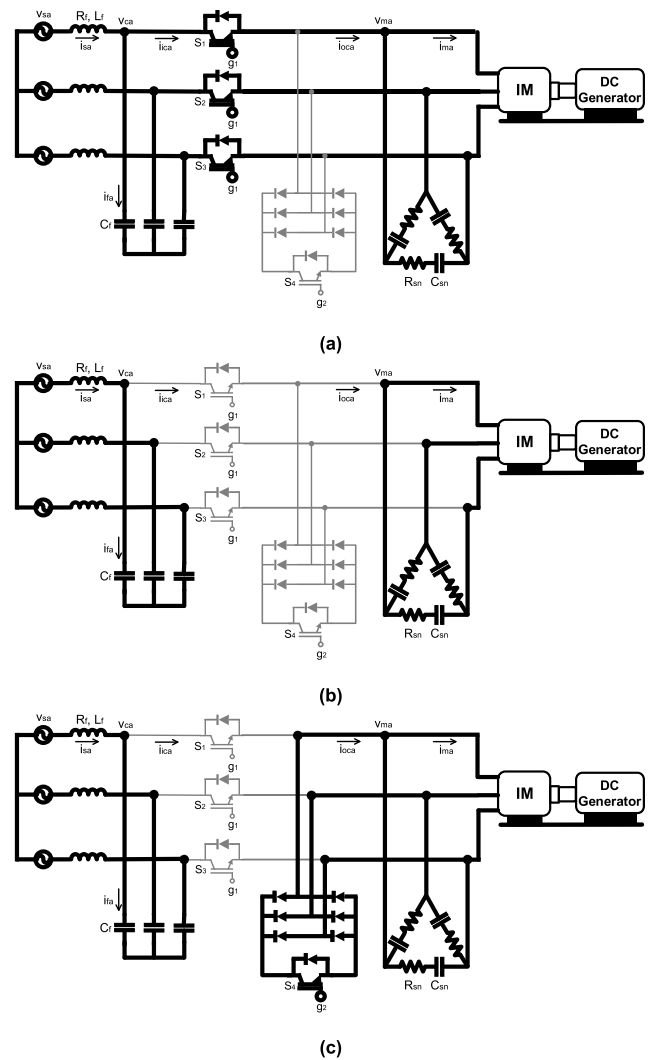


**FIGURE 2.** The currents paths of the proposed PWM AC chopper fed IM. (a) Active stage. (b) Dead time stage. (c) Freewheeling stage.

all four devices are turned OFF. The currents paths of the proposed PWM AC chopper fed IM in its three operating stages are illustrated by Fig. 2. A three phase Δ-connected snubber circuit, which has a resistance $R_{sn}$ and a capacitance $C_{sn}$ per phase, is used to minimize high voltage spikes at IM terminals due to switching of the chopper as well as providing the current path of IM during the dead time period. The input filter is composed of three inductors (whose resistance is $R_f$ and inductance is $L_f$ per phase) and Y-connected three capacitors (whose capacitance $C_f$ per phase). The LC input filter is used with the proposed PFC technique in order to reduce the harmonics of the supply current due to switching of the chopper. The proposed control circuit only generates two PWM complementary gate pulses ($g_1$ and $g_2$) which are used to drive the chopper IGBTs in order to provide the three main tasks of the proposed control strategy.

## III. PROPOSED CONTROL STRATEGY

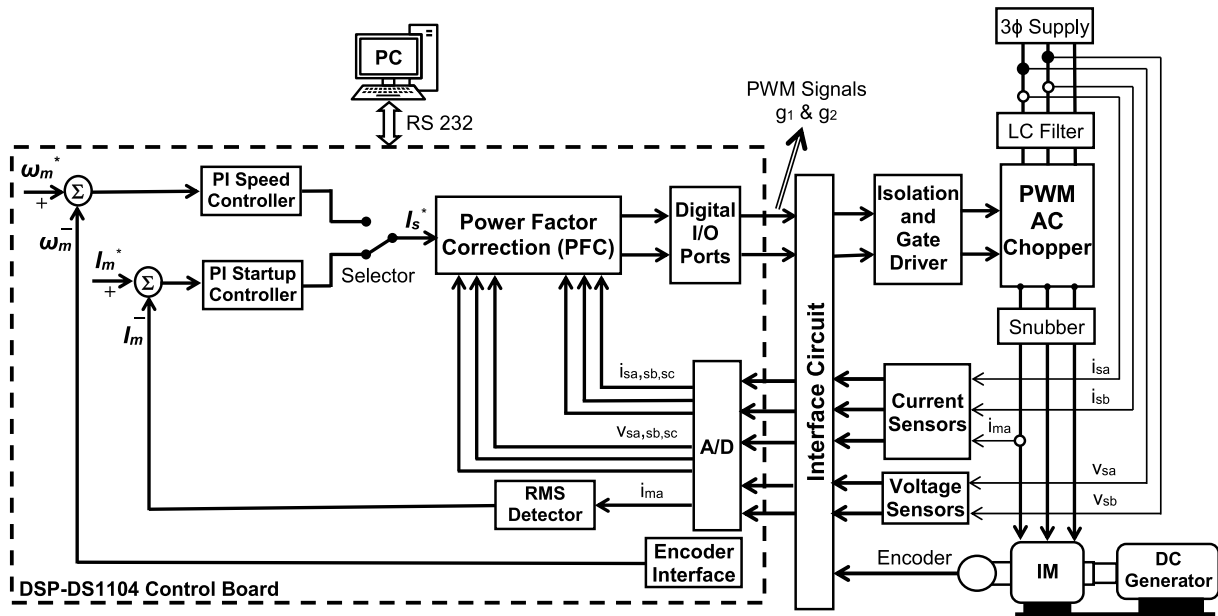The proposed control strategy has three main control objectives: soft starting, speed control, and input power factor

**FIGURE 3.** Block diagram of the proposed control circuit.

correction (PFC). This strategy is depending on the control of the applied voltage across IM terminals using AC chopper. Fig. 3 illustrates the schematic diagram of the proposed control strategy. It has two control loops. The inner control loop uses HBCC to force the chopper actual current signals to track their command current signals to achieve input PFC, whereas the outer control loop determines the magnitude of the reference currents either from starting mode or speed control mode. As a result, the inner loop controls the phase and the outer loop controls the magnitude of the chopper currents. In the first, the soft starting mode is working, and by giving a switching pulse to the selector switch, the speed control mode is activated and the soft starting mode is turned off.

## A. SOFT STARTING MODE

The role of the soft starting mode is to generate the reference value of the supply current in a manner that limits the starting current of the IM at a preset value. The actual current of IM ($I_m$) is measured and its RMS value is evaluated by RMS detector. The command or preset value of the motor current ($I_m^*$) and its actual value ($I_m$) are compared. The comparison resulted error is passed into a proportional integral (PI) controller to generate the command motor current ($I_s^*$). Limiting the starting current provides a smooth acceleration and reduces the torque pulsations of IM during soft starting period.

## B. SPEED CONTROL MODE

There are several methods for controlling the speed of three-phase IMs. These methods can be classified into two main categories according to the control side of the IM: a) speed control methods through the stator such as changing

the applied frequency, changing the applied voltage, changing the number of the stator poles and voltage/frequency (v/f) control, and b) speed control methods through the rotor such as rotor resistance control and rotor slip power recovery. Variable frequency drives (VFDs) are the commercial drives. Speed control by VFDs is based on changing both the stator voltage and frequency of the IM. VFDs are widely used for wide-range variable-speed IM applications. However, they are very expensive and hence not convenient when they are used for limited-range variable-speed IM applications. Since the proposed speed control strategy depends on changing the stator voltage only, so it is simple, low cost and more convenient for limited-range variable-speed IM application which is intended in this research. The role of the speed control mode is to generate the reference current value ($I_s^*$) in a way that makes the measured speed of IM ($\omega_m$) follows the command speed ($\omega_m^*$). Command and measured speed are compared and the difference is used as an input signal to a PI speed controller to generate $I_s^*$.

## C. PFC CONTROL

Since PWM AC/AC choppers can only modify the magnitude of the applied voltage, they are normally negatively viewed; when they are used in IM drive systems, for their low PF. Therefore, the main contribution of the proposed control strategy is achieving high PF approximately unity as in case of resistive loads. The proposed PFC strategy was implemented during starting and speed control operating modes of IM drive while using AC chopper. The principle of harmonic minimization of the proposed control strategy depends on using PWM technique. Whereas, the principle of reactive power management is to obtain PFC depends on
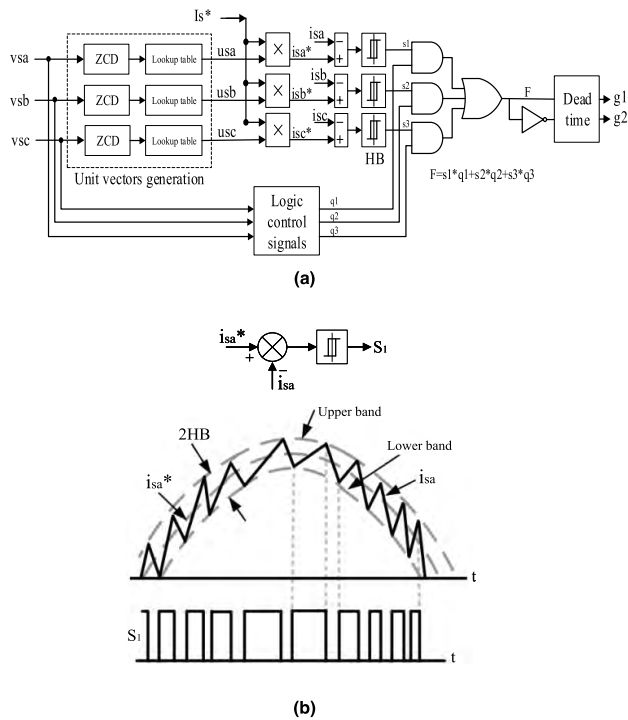
(a)



(b)

**FIGURE 4.** a) Proposed PFC using HBCC technique, (b) Generation of switching signal $S_1$.



(a)



(b)

**FIGURE 5.** (a) Switching frequency, (b) Frequency response of the LC input filter.

the proposed current control technique; in which the actual supply currents are forced to track their reference currents that are in phase with supply voltages. The role of PFC block is to continuously correct the input PF during IM operation. Fig. 4a shows the proposed PFC using HBCC technique. The reference value of the stator current ($I_s^*$) is utilized to obtain the three phase reference supply currents ($i_{sa}^*$, $i_{sb}^*$ and $i_{sc}^*$) by multiplying the value ($I_s^*$) by unit vectors of the supply voltages ($u_{sa}$, $u_{sb}$ and $u_{sc}$) as:

$$\begin{bmatrix} i_{sa}^* \\ i_{sb}^* \\ i_{sc}^* \end{bmatrix} = I_s^* \begin{bmatrix} 1 & 0 & 0 \\ 0 & 1 & 0 \\ 0 & 0 & 1 \end{bmatrix} \begin{bmatrix} u_{sa} \\ u_{sb} \\ u_{sc} \end{bmatrix} \qquad (1)$$

The unit vectors ($u_{sa}$, $u_{sb}$ and $u_{sc}$) are generated by measuring the phase voltages of the supply ($v_{sa}$, $v_{sb}$ and $v_{sc}$) and by using three zero crossing detection (ZCD) circuits and three lookup tables as shown in Fig. 4a. The reference currents of the supply ($i_{sa}^*$, $i_{sb}^*$ and $i_{sc}^*$), are compared with their corresponding actual values ($i_{sa}$, $i_{sb}$ and $i_{sc}$) respectively. The resulted errors are passed through three hysteresis bands (HBs) and their outputs are the three switching signals ($S_1$, $S_2$ and $S_3$). Operation of HBCC technique to obtain the switching signal ($S_1$) is explained by Fig. 4b. The logic control signals block is utilized to find the higher value of the supply phase voltages. The switching signal $F$ is generated from the three switching signals ($S_1$, $S_2$ and $S_3$) and the three logic control signals ($q1$, $q2$ and $q3$) as:

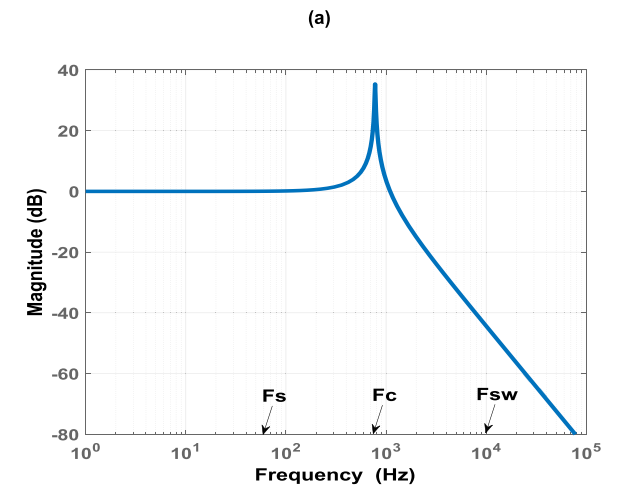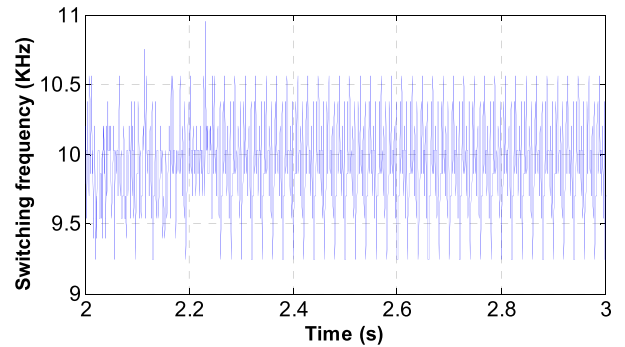$$F = S_1 \times q1 + S_2 \times q2 + S_3 \times q3 \qquad (2)$$

The switching signal $F$ and its complementary signal are passed through a dead time block in order to obtain the two PWM complementary signals ($g_1$ and $g_2$) that are used to drive the chopper IGBTs.

The idea of the proposed PFC technique is to force continuously the actual supply currents to follows their corresponding command currents which are in phase with supply voltages in both the two control modes. Considering a sinusoidal supply voltage, the *PF* at which a converter system operates is defined as follows:

$$PF = \frac{I_{s1}}{I_s} DPF \qquad (3)$$

where $I_s$ and $I_{s1}$ are the RMS values of the supply current and its first order component, respectively. *DPF* is the displacement power factor that equals the cosine of the angle by which the first order component of the current is displaced with respect to the input voltage wave.

However, $I_{S1}/I_S$ (i.e. the distortion factor) is the ratio of the RMS value of the first order component to the RMS value the supply current Is; which can be calculated as follows:

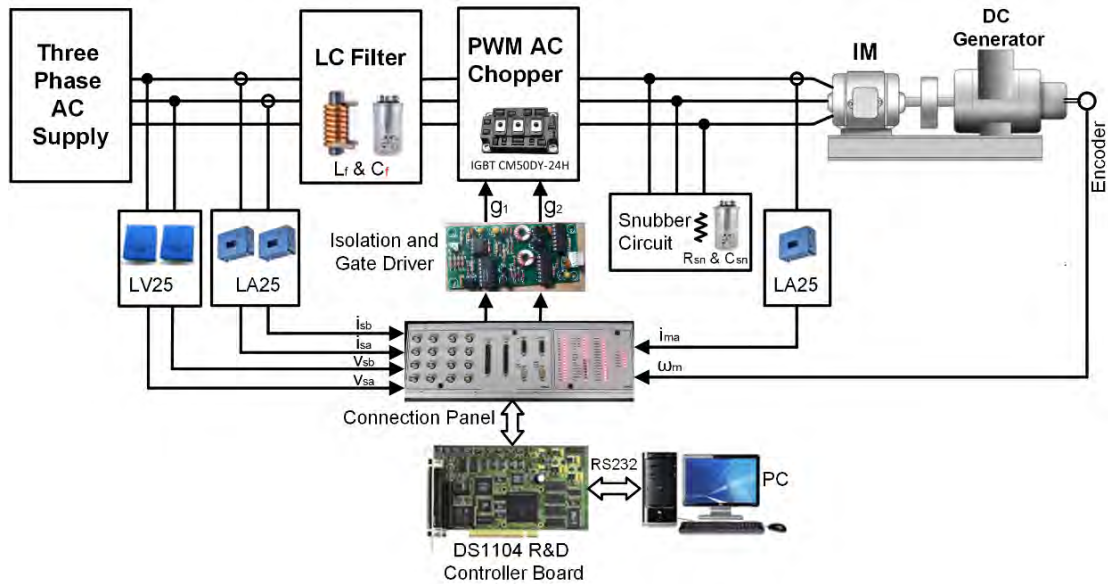$$I_s = \sqrt{I_{s1}^2 + \sum_{h=2}^{\infty} I_{sh}^2} \qquad (4)$$

**FIGURE 6.** Schematic diagram of the experimental setup.

From (4), the RMS value of the distortion component can be written as:

$$I_{dis} = \sqrt{I_s^2 - I_{s1}^2} = \sqrt{\sum_{h=2}^{\infty} I_{sh}^2} \qquad (5)$$

However, the percentage total harmonics distortion (*THD*) is defined as:

$$THD = \frac{I_{dis}}{I_{s1}}\% \qquad (6)$$

From (3), (4) and (6), the *PF* can be written as:

$$PF = \frac{1}{\sqrt{1 + \left(\frac{THD}{100}\right)^2}} \cdot DPF \qquad (7)$$

Thus, the DPF should be high and the THD should be low to yield a higher input PF. These factors (DPF and THD) are controlled using the proposed PFC control.

## IV. MATHEMATICAL ANALYSIS
The mathematical analysis of the proposed AC chopper, LC input filter, and the three-phase squirrel-cage IM are discussed in the following subsections.

### A. ANALYSIS of THE PROPOSED AC CHOPPER
The three-phase supply voltages can be defined as:

$$\begin{bmatrix} v_{sa} \\ v_{sb} \\ v_{sc} \end{bmatrix} = V_m \begin{bmatrix} 1 & 0 & 0 \\ 0 & 1 & 0 \\ 0 & 0 & 1 \end{bmatrix} \begin{bmatrix} \sin(\omega t) \\ \sin(\omega t - 120°) \\ \sin(\omega t - 240°) \end{bmatrix} \qquad (8)$$

where $V_m$ is the peak value of the supply voltage and its angular frequency is $\omega$. The supply voltages are chopped by the power regulating switches ($S_1$, $S_2$ and $S_3$). Variation of the duty ratio for IGBT switches of the AC chopper is utilized to change the effective values of the voltage and hence the

current of IM. Increasing the duty ratio will allow the value of the input voltage to increase. While reducing the duty ratio reduces the value of the input voltage. The IM input voltage is calculated using the following equation:

$$v_M(t) = DV_m \sin(\omega t) \qquad (9)$$

where the duty ratio is *D*. Equation (9) illustrates that the IM voltage is mainly depending on the duty ratio of the PWM AC chopper. The duty ratio can be given by:

$$D = \frac{T_{on}}{T_{sw}} = \frac{T_{on}}{T_{on} + T_{off}} \qquad (10)$$

where $T_{on}$ is the on time, $T_{off}$ is the off time and $T_{sw}$ is the switching time period. The switching frequency ($F_{sw}$) is given by:

$$F_{sw} = \frac{1}{T_{sw}} \qquad (11)$$

In the active stage, the power semiconductor devices ($S_1$, $S_2$ and $S_3$) are ON and the power device $S_4$ is OFF. Therefore, the following equations can be derived:

$$\begin{bmatrix} v_{ma} \\ v_{mb} \\ v_{mc} \end{bmatrix} = \begin{bmatrix} 1 & 0 & 0 \\ 0 & 1 & 0 \\ 0 & 0 & 1 \end{bmatrix} \begin{bmatrix} v_{ca} \\ v_{cb} \\ v_{cc} \end{bmatrix} \qquad (12)$$

where $v_{ma}$, $v_{mb}$, $v_{mc}$ are the three phase motor voltages, and the input voltages to the AC chopper are $v_{ca}$, $v_{cb}$, $v_{cc}$. In the freewheeling stage, the power switch $S_4$ is ON and the regulating power switches are OFF. The voltages on the IM terminals are zero as a result we can write

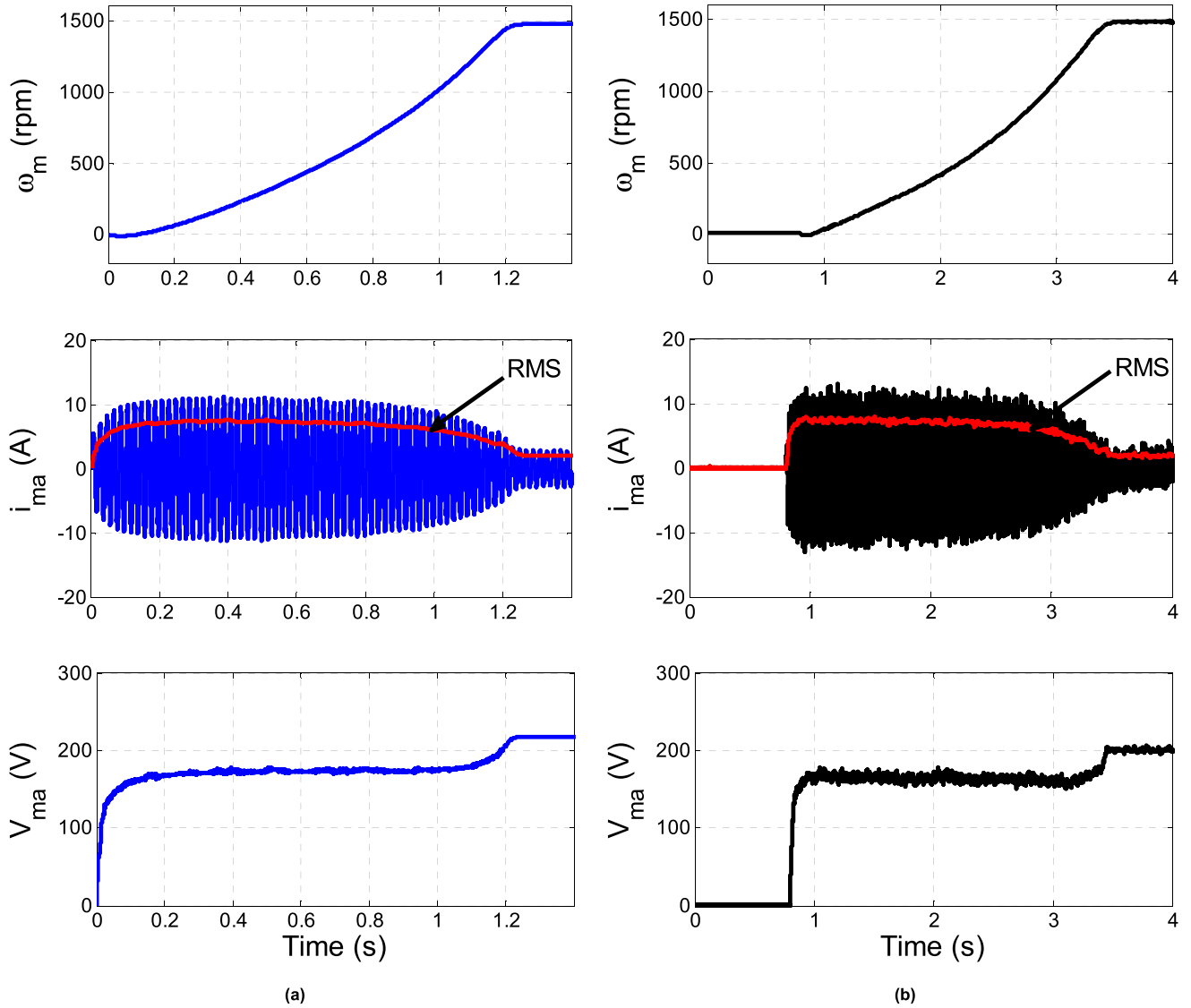$$v_{ma} + v_{mb} + v_{mc} = 0 \qquad (13)$$

**FIGURE 7.** Starting of the motor with the proposed PWM AC chopper. (a) Simulation. (b) Experimental.

## B. ANALYSIS OF THE LC INPUT FILTER

The theoretical analyses of the LC input filter are described using the following equations as in [26]:

$$\begin{bmatrix} v_{sa} \\ v_{sb} \\ v_{sc} \end{bmatrix} = \begin{bmatrix} R_f + L_f p & 0 & 0 \\ 0 & R_f + L_f p & 0 \\ 0 & 0 & R_f + L_f p \end{bmatrix} \begin{bmatrix} i_{sa} \\ i_{sb} \\ i_{sc} \end{bmatrix}$$
$$+ \begin{bmatrix} v_{ca} \\ v_{cb} \\ v_{cc} \end{bmatrix} \tag{14}$$

$$\begin{bmatrix} v_{ca} \\ v_{cb} \\ v_{cc} \end{bmatrix} = \frac{1}{C_f} \begin{bmatrix} 1 & 0 & 0 \\ 0 & 1 & 0 \\ 0 & 0 & 1 \end{bmatrix} \begin{bmatrix} \int i_{fa} dt \\ \int i_{fb} dt \\ \int i_{fc} dt \end{bmatrix} \tag{15}$$

$$\begin{bmatrix} i_{sa} \\ i_{sb} \\ i_{sc} \end{bmatrix} = \begin{bmatrix} 1 & 0 & 0 \\ 0 & 1 & 0 \\ 0 & 0 & 1 \end{bmatrix} \begin{bmatrix} i_{ica} \\ i_{icb} \\ i_{icc} \end{bmatrix} + \begin{bmatrix} 1 & 0 & 0 \\ 0 & 1 & 0 \\ 0 & 0 & 1 \end{bmatrix} \begin{bmatrix} i_{fa} \\ i_{fb} \\ i_{fc} \end{bmatrix} \tag{16}$$

where $i_{Sa}$, $i_{Sb}$, $i_{Sc}$ are the supply line currents; $R_f$ is the input filter resistance, $L_f$ is the inductance of input filter and $C_f$ is the capacitance of the input filter; $p$ is the differentiation operator. The filter capacitors currents are $i_{fa}$, $i_{fb}$, $i_{fc}$; and the chopper line currents are $i_{ca}$, $i_{cb}$, $i_{cc}$. The variation of the supply currents ($i_{sa}$, $i_{sb}$, $i_{sc}$) is evaluated by the input filter and the IM parameters.

Since the proposed topology depends on the capacitance of the LC filter, so analysis of the capacitance ripple current is essential. In order to study the ripple current of the capacitance, the filter current ($i_{fa}$) for phase a can be separated into two components; average component ($\bar{i}_{fa}$) and ripple component ($\tilde{i}_{fa}$) as follow:

$$i_{fa} = \bar{i}_{fa} + \tilde{i}_{fa} \tag{17}$$

The rms value of the ripple component of the filter capacitance current ($\tilde{I}_{fa,rms}$) phase a can be derived approximately
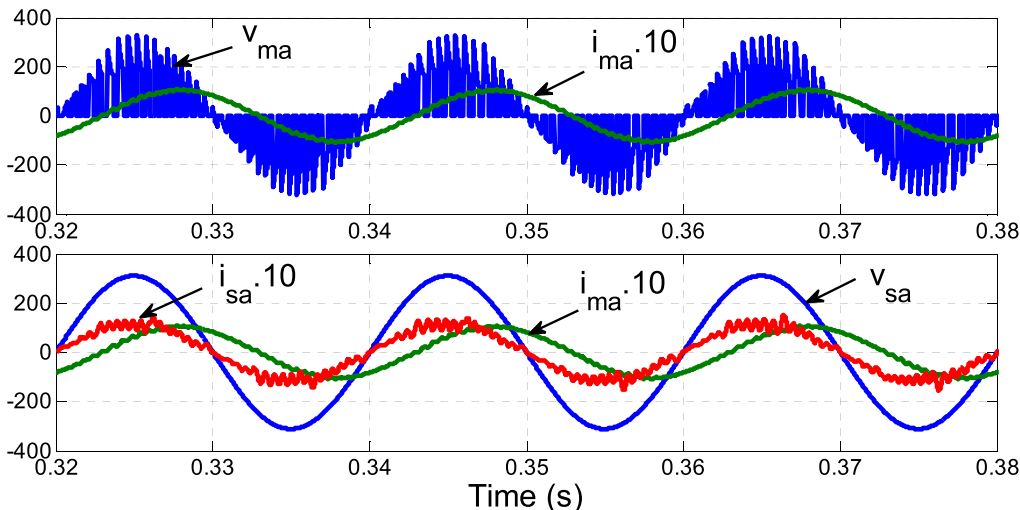
**FIGURE 8.** PFC of the drive system during start-up of the IM.

as follows [32]:

$$\tilde{I}_{fa,rms} = I_{oca}\sqrt{D(1-D)} \qquad (18)$$

where $I_{oca}$ is the rms value of phase a chopper output current.

Parameters design of the LC input filter depends on its cut-off frequency ($F_c$) that can be given as:

$$F_c = \frac{1}{2\pi\sqrt{L_f C_f}} \qquad (19)$$

Proper selection of the cut-off frequency will properly filter out the input pulsating current resulting from the chopper switching. The cut-off frequency should fulfill the following relation:

$$F_s \ll F_c \ll F_{sw} \qquad (20)$$

where $F_s$ and $F_{sw}$ are the supply and the switching frequencies, respectively. The cut-off frequency ($F_c$) should be selected 10–20 times lower than the switching frequency ($F_{sw}$) of the PWM AC chopper in order to suppress effectively the high-order harmonics of the input current and, at the same time, higher than the fundamental frequency of the supply; i.e. 50 Hz. Since the average switching frequency of the chopper is 10 KHz as seen in Fig. 5a, the parameters of LC filter have been taken as: $L_f = 6$ mH, $R_f = 0.5$ Ω, and $C_f = 7$ μF, and hence the cut-off frequency of the LC input filter is equal to 776.6 Hz; about 13 times lower than the switching frequency. The frequency response of the designed low-pass second-order LC input filter is seen in Fig. 5b.

## C. IM MODEL

The equations of the IM in quadrature and direct ($q - d$) axes synchronously rotating reference frame are presented as

follows:

$$\begin{bmatrix} v_{qs}^e \\ v_{ds}^e \\ v_{qr}^e \\ v_{dr}^e \end{bmatrix} = \begin{bmatrix} R_S & 0 & 0 & 0 \\ 0 & R_S & 0 & 0 \\ 0 & 0 & R_r & 0 \\ 0 & 0 & 0 & R_r \end{bmatrix} \begin{bmatrix} i_{qs}^e \\ i_{ds}^e \\ i_{qr}^e \\ i_{dr}^e \end{bmatrix} + \begin{bmatrix} \frac{d\lambda_{qs}^e}{dt} \\ \frac{d\lambda_{ds}^e}{dt} \\ \frac{d\lambda_{qr}^e}{dt} \\ \frac{d\lambda_{dr}^e}{dt} \end{bmatrix}$$
$$+ \begin{bmatrix} \omega_s\lambda_{ds}^e \\ -\omega_s\lambda_{qs}^e \\ (\omega_s - \omega_r)\lambda_{dr}^e \\ -(\omega_s - \omega_r)\lambda_{qr}^e \end{bmatrix} \qquad (21)$$

where;

$$\begin{bmatrix} \lambda_{qs}^e \\ \lambda_{ds}^e \\ \lambda_{qr}^e \\ \lambda_{dr}^e \end{bmatrix} = \begin{bmatrix} L_s & 0 & L_m & 0 \\ 0 & L_s & 0 & L_m \\ L_m & 0 & L_r & 0 \\ 0 & L_m & 0 & L_r \end{bmatrix} \begin{bmatrix} i_{qs}^e \\ i_{ds}^e \\ i_{qr}^e \\ i_{dr}^e \end{bmatrix} \qquad (22)$$

where $L_s = L_{ls} + L_m$, and $L_r = L_{lr} + L_m$. The electrical torque is given by;

$$T_e = \frac{3}{2}\left(\frac{P}{2}\right)L_m\left(i_{qs}^e i_{dr}^e - i_{ds}^e i_{qr}^e\right) \qquad (23)$$

The motion equation can be given as:

$$T_e = J\frac{d\omega_r}{dt} + \beta\omega_r + T_L \qquad (24)$$

where $\mathbf{v_{qs}^e}$ and $\mathbf{v_{ds}^e}$ are ($q-d$) axes stator voltages respectively, the stator currents in q-d are $\mathbf{i_{qs}^e}$ and $\mathbf{i_{ds}^e}$, the rotor currents in $q - d$ are $\mathbf{i_{qr}^e}$ and $\mathbf{i_{dr}^e}$, the stator flux linkages in q-d are $\mathbf{\lambda_{qs}^e}$ and $\mathbf{\lambda_{ds}^e}$, the rotor flux linkages in $q - d$ are $\mathbf{\lambda_{qr}^e}$ and $\mathbf{\lambda_{dr}^e}$, $\mathbf{R_S}$ and $\mathbf{R_r}$ are the IM stator and rotor resistances, $\mathbf{L_m}$ is the IM mutual inductance, $\mathbf{L_s}$ and $\mathbf{L_r}$ are the IM stator and rotor self-inductances. $T_e$ and $T_L$ are the IM electrical torque and mechanical load torque respectively, $\mathbf{P}$ is pole numbers, and $\omega_r$ is the IM electrical rotor speed. The moment of inertia and viscous frictions parameters are $J$ and $\beta$, respectively.
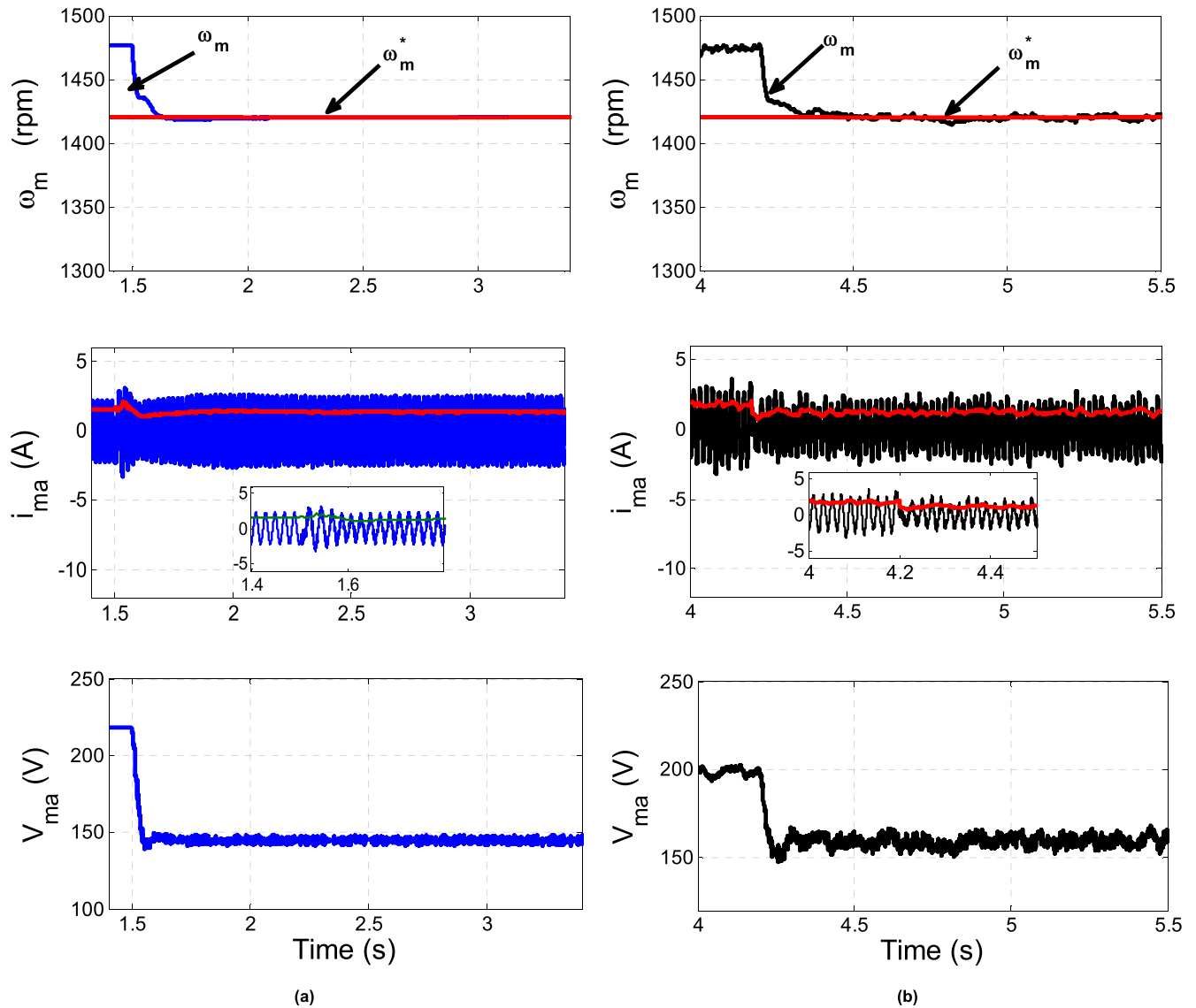
**FIGURE 9.** Variation of the motor speed, current and phase voltage at activation of the speed controller. (a) Simulation. (b) Experimental.

## V. HARDWARE IMPLEMENTATION

To validate and verify the simulations of the proposed control strategy, a laboratory system of the proposed control strategy was implemented and runs under different operating states. Fig. 6 shows the schematic diagram of the laboratory system, including an input filter, AC chopper, snubber circuit, three phase IM coupled with DC generate as a load, a digital signal processing control board dSPACE (DS1104) and IGBT gate driver. AC chopper switches $S_1$, $S_2$, $S_3$ and $S_4$ are 50A/1200V IGBT MITSUBISHI Module (CM50DY-24H). The required pulses ($g_1$ and $g_2$) are generated by using a digital signal processing control board (DS1104) synchronized with MATLAB/SIMULINK environment. A gate interface board circuit is connected between the outputs of digital signal control board (DS1104) and the IGBTs to obtain pulses of nearly 15 V to enforce effective IGBT switching states. The three phase supply voltages ($V_{Sa,b,c}$), three phase

supply currents ($i_{Sa,b,c}$) and motor phase current ($i_{ma}$) are measured using voltage and current sensors and sent their signals to the digital signal control board (DS1104) through the analog to digital converter ports. The IM speed ($\omega_m$) is measured by position encoder (HENGSTLER) connected to rotor shaft of IM. The DSP-DS1104 control board has facilitates to capture the experimental data and export them numerically per sample. The DSP-DS1104 board can record the experimental waveforms as capture images or MATLAB files (.mat). Since the captured images have a low resolution, so the experimental waveforms are plotted with MATLAB program to obtain figures with a high resolution.

## VI. RESULTS

The proposed AC chopper is simulated in the MATLAB/ Simulink environment and a prototype model is implemented. The simulation was used to confirm the proposed control
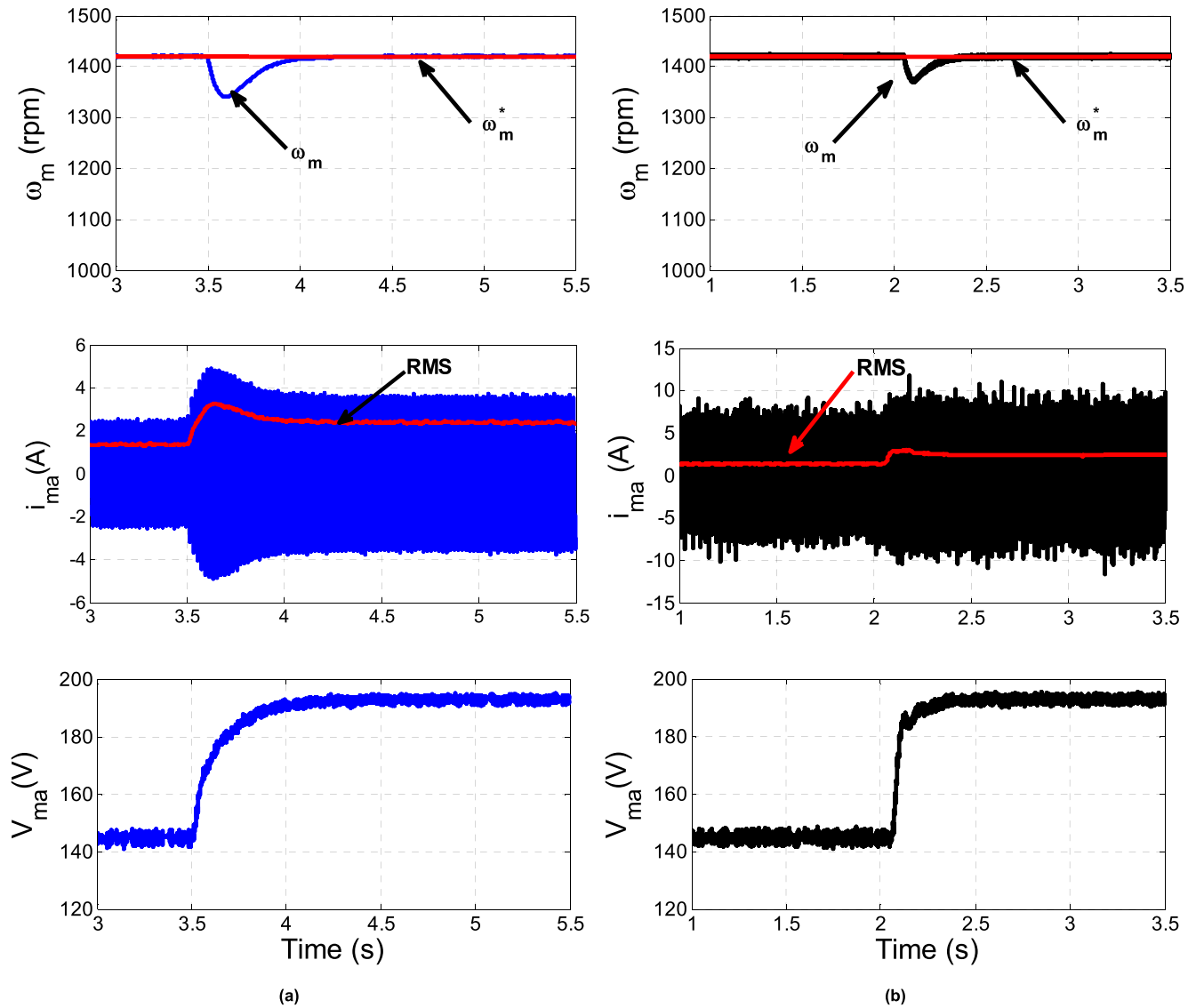
**FIGURE 10.** Variation of the motor speed, current and phase voltage at step change in the load torque. (a) Simulation. (b) Experimental.

strategy theoretically. While the experimental prototype has been constructed to confirm the proposed strategy experimentally. Four test cases are examined. Corresponding simulation and experimental results are obtained and compared. Parameters of the system under study are given in the appendix.

### A. CASE 1: STARTING OF THE MOTOR
In this test case, the motor is started with the proposed control strategy (soft starting mode) at load torque ($T_L$) equal to 25% of the rated torque ($T_L = 1.75$ N.m), and $I_m^* = 7.5$A which is 2 times of the rated motor current. Fig. 7 illustrates the motor speed ($\omega_m$), motor phase-a current ($i_{ma}$), and RMS motor phase-a voltage ($V_{ma}$) responses during starting, respectively. As seen, the rise of the motor phase voltage is controlled during the starting period in order to restrict the starting current at the predetermined level; 2 times of the rated current. Furthermore, the motor speed has a smooth acceleration. So,

soft startup of the motor is achieved avoiding the electrical and mechanical drawbacks of the direct online (DOL) starting and hence the motor life is increased.

Fig. 8 illustrates the instantaneous waveforms of the chopped motor voltage ($v_{ma}$), motor current ($i_{ma}$), supply voltage ($v_{sa}$), and supply current ($i_{sa}$) during startup of the IM. As seen from the results, the motor current lags the motor voltage due to the inductance of the IM windings. Whereas, by the help of the proposed HBCC technique, the supply current ($i_{sa}$) is forced to be in phase with the supply voltage ($v_{sa}$) regardless the inductive load type of IM making the input PF of the drive system to be approximately unity.

### B. CASE 2: ACTIVATION THE SPEED CONTROLLER
Fig. 9 shows the motor speed, current and phase voltage responses when the speed control mode is launched.
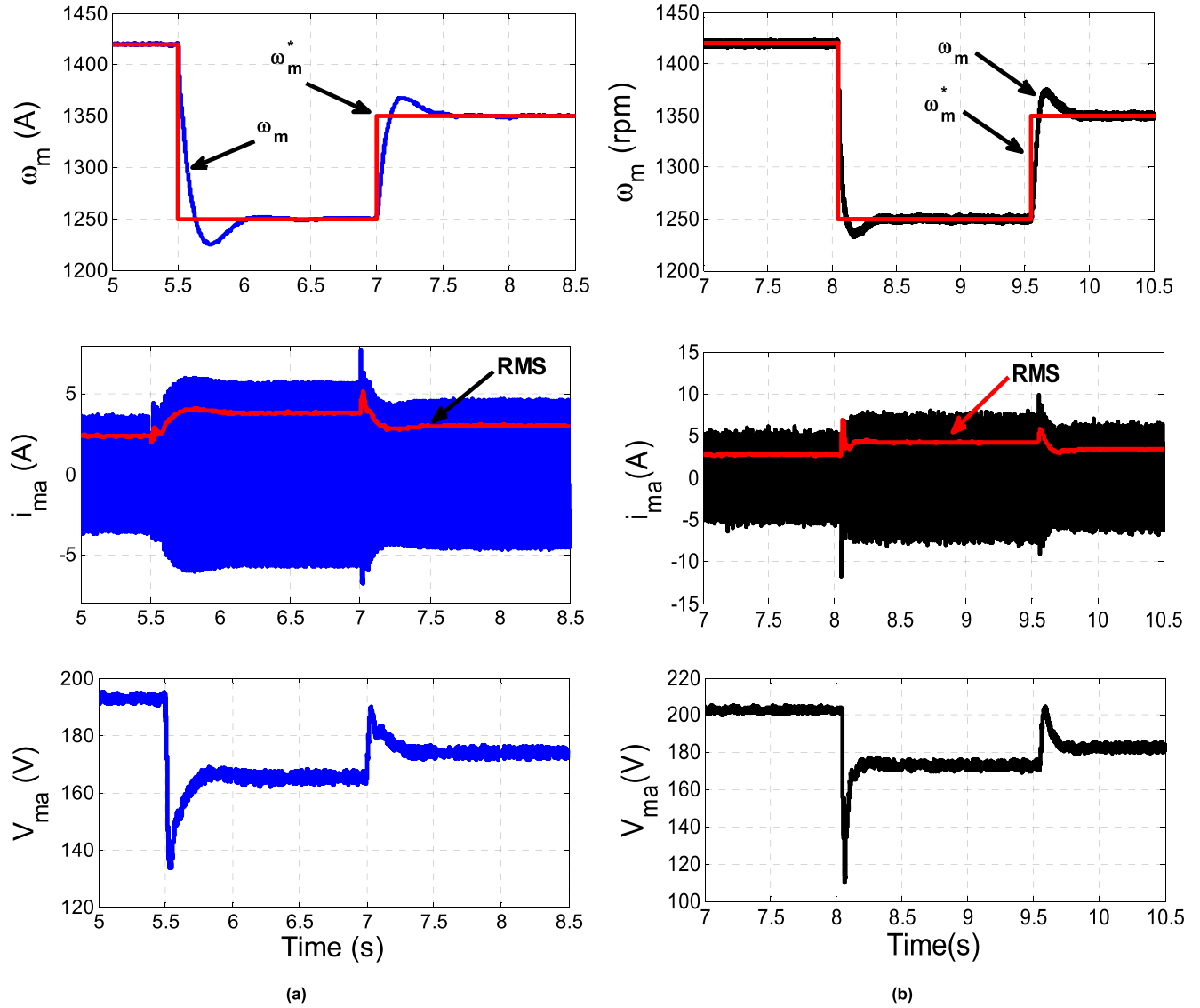
**FIGURE 11.** Variation of the motor speed, current and phase voltage at step change in the reference speed. (a) Simulation. (b) Experimental.
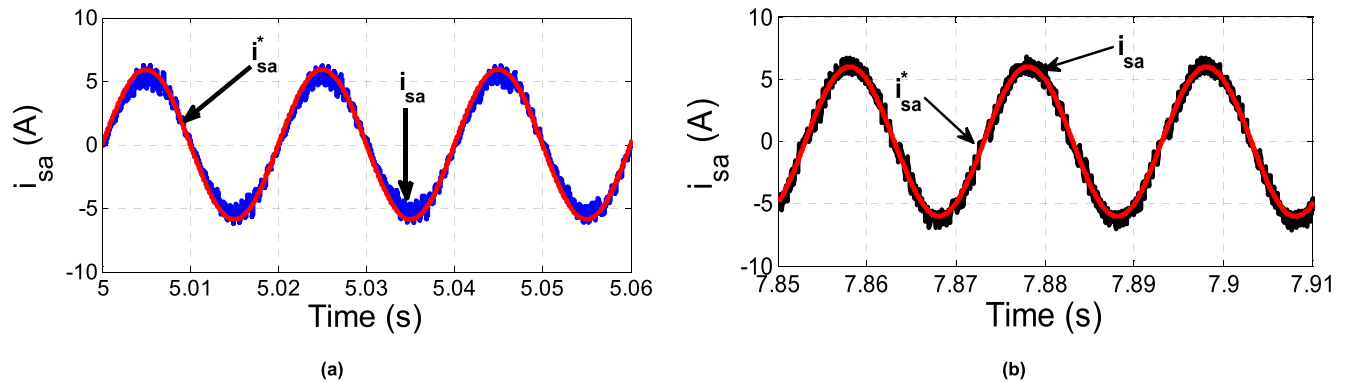


**FIGURE 12.** Reference and measured currents of the supply. (a) Simulation. (b) Experimental.

This mode is activated in simulation at time $t = 1.5$ s with speed reference ($\omega_m^*$) 1420 rpm and load torque $T_L = 25\%$ of rated load torque (1.75 N.m). It is clear from the illustrated

waveforms in Fig. 9 that the motor speed effectively tracks its reference value. Also, the motor voltage and hence the current decreases with decreasing the motor speed. The experimental
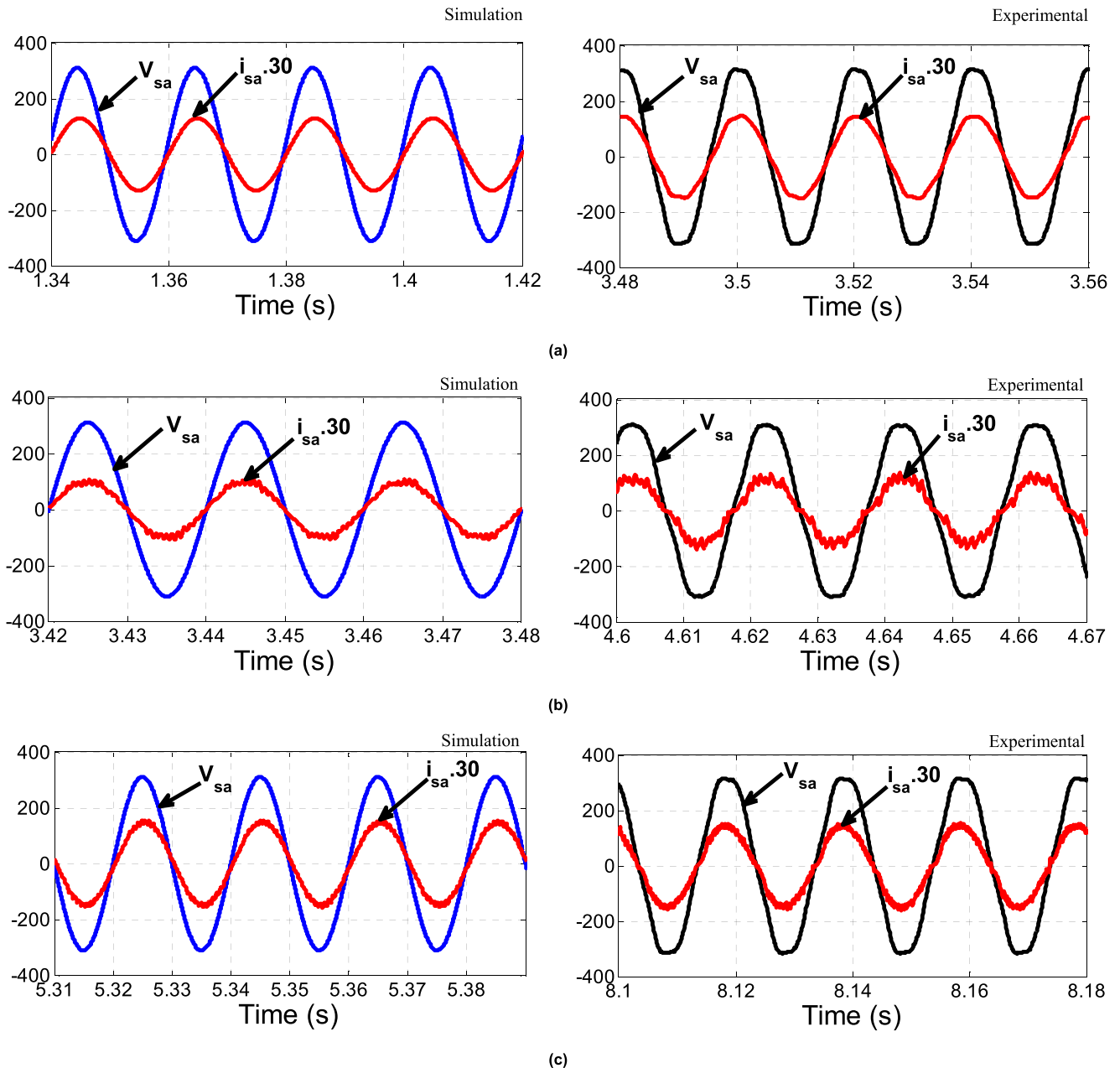
**FIGURE 13.** Supply voltage and current at different testing cases of the proposed system. (a) Case 1. (b) Case 2. (c) Case 3.

results are similar to simulation results and verify the validation of the proposed control algorithm.

### C. CASE 3: STEP CHANGE IN THE MOTOR LOAD TORQUE
Variation of the motor speed, current and phase voltage at step change in the load torque from 25% (1.75 N.m) to 80% (5.6 N.m) of rated load torque are illustrated in Fig. 10. As seen from the waveforms, the motor current and voltage increase with increasing the load torque. Also, the motor speed decreases with increasing the load torque and returns back quickly to its command value which proves the effectiveness of the proposed speed controller versus sudden loading with 80% of full load torque.

### D. CASE 4: STEP CHANGE IN THE REFERENCE SPEED
Fig. 11 shows the motor speed, current and phase voltage responses at step change of the reference speed. In this case, at 80% full load torque, the system is subjected to a step decrease of the reference speed from 1420 rpm to 1250 rpm followed by a step increase in the reference speed from 1250 rpm to 1350 rpm as shown in Fig. 11. It is clear from the results that the speed controller is robust and effective as the actual motor speed ($\omega_m$) tracks the variations in the reference speed ($\omega_m^*$) quickly with a minimum steady state error.

Fig. 12 shows the simulation and experimental results of the reference and measured currents of the supply. It is clear that the measured current follows the reference current in a

certain band. This proves the effectiveness of the proposed HBCC strategy.

The simulated and experimented waveforms of $v_{sa}$ and $i_{sa}$ for the first three testing cases; case 1, case 2 and case 3, are presented in Fig. 13. As illustrated, the simulated and experimental results are in a close agreement, the supply currents are approximately sinusoidal and are in phase with the corresponding supply voltages during all the test cases which ensure that the input PFC is achieved and hence prove the validity of the proposed current control strategy. The drawback of the proposed PWM AC chopper fed IM is that it is one quadrant converter. Therefore, it has not the ability to reverse the speed direction of the motor nor to handle with the negative load torque.

### E. THD AND PF COMPARISON
The performance of IM without PFC is roughly compared in accordance with concerning the proposed PFC technique. Regarding the technical performance that can be summarized from the previous study, Table 1 shows the THD and PF values are used in the comparison evaluation. From the results in this table, the PF of IM without control of the proposed PFC strategy is low. Also, the control with PFC has better performance during soft starting, speed control and loading conditions. With evaluating PF using simulation and experiments, the PF for case 1 has 0.99999 and 0.9998 respectively, also the PF for case 2 has 0.99597 and 0.9982 respectively, while the PF for case 3 has 0.99756 and 0.99857 respectively.

**TABLE 1.** THD and PF at Different Cases.

| Face of comparison | | Without PFC | PFC case1 | PFC case2 | PFC case3 |
|---|---|---|---|---|---|
| THD | Simulation | THD=0%, θ=50° | 3% | 9 % | 7 % |
| | Experimental | THD=1.6%, θ=46° | 2 % | 6 % | 5 % |
| PF | Simulation | 0.6427 | 0.99999 | 0.99597 | 0.99756 |
| | Experimental | 0.695 | 0.9998 | 0.9982 | 0.99857 |

## VII. CONCLUSION
A new control strategy of three-phase squirrel cage IM fed from PWM AC chopper has been simulated and laboratory implemented using dSPACE (DS1104) control board. The main control objective is to correct the input PF with different operating conditions of the induction motor drive system. Input PFC is achieved by forcing the actual currents of the chopper to track their reference currents that are in phase with the input voltages using HBCC technique. The proposed control strategy uses only two PWM signals for driving the active switches of the AC chopper. The proposed system is simple, reliable and low cost as it has only four IGBT switches. Operation principle and mathematical analysis of the proposed system are introduced. The system was simulated using MATLAB/SIMULINK and a laboratory system was implemented. The effectiveness of the proposed control

strategy has been tested at starting, reference speed change and load torque variation. The obtained results from the experimental and computer simulation works verify the validity of the proposed control strategy during all testing conditions. Performance of the system without PFC is roughly compared in accordance with concerning the proposed PFC technique during the three test cases. Comparative results illustrate that the system with the proposed PFC technique has a corrected PF and hence a better performance.

## APPENDIX
See Table 2.

**TABLE 2.** Parameters of the System.

| Symbol | PARAMETER | Value |
|---|---|---|
| $V_s$ | supply voltage | 220 V |
| $f$ | Line frequency | 50 Hz |
| $R_f$ | filter resistor | 0.5 Ω |
| $L_f$ | filter inductor | 6 mH |
| $C_f$ | filter capacitance | 7 μF |
| $V_s$ | IM rated voltage | 220 V/ph |
| $P_o$ | rated power of IM | 1.5 hp |
| $N$ | IM rated speed | 1420 rpm |
| $P$ | No. of poles | 4 |
| $T_l$ | Rated load torque | 7 N.m |
| $R_s$ | Stator winding resistance | 7.4826 Ω/ph |
| $L_{ls}$ | Stator leakage inductance | 0.0221 H/ph |
| $R_r$ | Rotor winding resistance | 3.6840 Ω/ph |
| $L_{lr}$ | Rotor leakage inductance | 0.0221 H/ph |
| $L_m$ | Mutual inductance | 0.4114 H |
| $\beta$ | Motor friction | 0.008 |
| $J$ | IM moment of inertia | 0.02 kg.m$^2$ |

### REFERENCES
[1] T. Mishima, Y. Nakagawa, and M. Nakaoka, "A bridgeless BHB ZVS-PWM AC–AC converter for high-frequency induction heating applications," *IEEE Trans. Ind. Appl.*, vol. 51, no. 4, pp. 3304–3315, Jul./Aug. 2015. doi: 10.1109/TIA.2015.2409177.

[2] S. Mahendran, I. Gnanambal, and A. Maheswari, "FPGA-based genetic algorithm implementation for AC chopper fed induction motor," *Int. J. Electron.*, vol. 103, no. 12, pp. 2029–2041, Apr. 2016. doi: 10.1080/00207217.2016.1175034.

[3] F. Luo, H. Ye, and M. H. Rashid, *Digital Power Electronics and Applications*. Amsterdam, The Netherlands: Elsevier, 2005.

[4] L. Rajaji, C. Kumar, and M. Vasudevan, "Fuzzy and ANFIS based soft starter fed induction motor drive for high performance applications," *ARPN J. Eng. Appl. Sci.*, vol. 3, no. 4, pp. 12–24, Aug. 2008.

[5] A. Gastli and M. M. Ahmed, "ANN-based soft starting of voltage-controlled-fed IM drive system," *IEEE Trans. Energy Convers.*, vol. 20, no. 3, pp. 497–503, Sep. 2005. doi: 10.1109/TEC.2004.841522.

[6] M. Muchlas and H. Soetedjo, "Use of the maximum torque sensor to reduce the starting current in the induction motor," *Sensors Transducers*, vol. 114, no. 3, pp. 161–169, Mar. 2010.

[7] G. Zenginobuz, I. Cadirci, M. Ermis, and C. Barlak, "Performance optimization of induction motors during voltage-controlled soft starting," *IEEE Trans. Energy Convers.*, vol. 19, no. 2, pp. 278–288, Jun. 2004. doi: 10.1109/TEC.2003.822292.

[8] K. Sundareswaran and P. S. Nayak, "Ant colony-based feedback controller design for soft-starter fed induction motor drive," *Appl. Soft Comput.*, vol. 12, no. 5, pp. 1566–1573, May 2012. doi: 10.1016/j.asoc.2011.12.012.

[9] K. Sundareswaran, N. Rajasekar, and V. T. Sreedevi, "Performance comparison of capacitor-run induction motors supplied from AC voltage regulator and SPWM AC chopper," *IEEE Trans. Ind. Electron.*, vol. 53, no. 3, pp. 990–993, Jun. 2006. doi: 10.1109/TIE.2006.874256.

[10] S. Jothibasu and M. K. Mishra, "An improved direct AC–AC converter for voltage sag mitigation," *IEEE Trans. Ind. Electron.*, vol. 62, no. 1, pp. 21–29, Jan. 2015. doi: 10.1109/TIE.2014.2334668.

[11] Z. Chen, C. Mao, D. Wang, J. Lu, and Y. Zhou, "Design and implementation of voltage source converter excitation system to improve power system stability," *IEEE Trans. Ind. Appl.*, vol. 52, no. 4, pp. 2778–2788, Jul./Aug. 2016. doi: 10.1109/TIA.2016.2543685.

[12] D. Yildirim and M. Bilgic, "PWM AC chopper control of single-phase induction motor for variable-speed fan application," in *Proc. IEEE IECON*, Orlando, FL, USA, Nov. 2008, pp. 1337–1342.

[13] J. M. Flores-Arias, A. M. MuÃśoz, F. D. Perez, V. Pallares-Lopez, and D. Gutierrez, "Voltage regulator system based on a PWM AC chopper converter," in *Proc. IEEE ISIE*, Gdansk, Poland, Jun. 2011, pp. 468–473.

[14] K. Sundareswaran and A. P. Kumar, "Voltage harmonic elimination in PWM AC chopper using genetic algorithm," *IEE Proc. - Electric Power Appl.*, vol. 151, no. 1, pp. 26–31, Jan. 2004. doi: 10.1049/ip-epa:20040061.

[15] K. Georgakas and A. Safacas, "Modified sinusoidal pulse-width modulation operation technique of an AC–AC single-phase converter to optimise the power factor," *IET Power Electron.*, vol. 3, no. 3, pp. 454–464, May 2010. doi: 10.1049/iet-pel.2009.0092.

[16] D.-H. Jang and G.-H. Choe, "Improvement of input power factor in AC choppers using asymmetrical PWM technique," *IEEE Trans. Ind. Electron.*, vol. 42, no. 2, pp. 179–185, Apr. 1995. doi: 10.1109/41.370384.

[17] P. Sanjit and A. Aurasopon, "Asymmetrical PWM for harmonics reduction and power factor improvement in PWM AC choppers using bee colony optimization," *J. Power Electron.*, vol. 15, no. 1, pp. 227–234, Jan. 2015. doi: 10.6113/JPE.2015.15.1.227.

[18] A. Aurasopon, A. Aurasopon, and W. Khamsen, "Improvement of input power factor in PWM AC chopper by selecting the optimal parameters," *Przegląd Elektrotechniczny*, vol. 89, no. 10, pp. 210–216, 2013.

[19] N. A. Ahmed and E. H. El-Zohri, "Power factor improvement of single-phase AC voltage controller employing extinction angle control technique," in *Proc. 46th Midwest Symp. Circuits Syst.*, Cairo, Egypt, Dec. 2003, pp. 1075–1080.

[20] B. H. Kwon, B. D. Min, and J. H. Kim, "Novel topologies of AC choppers," *IEE Proc.-Electr. Power Appl.*, vol. 143, no. 4, pp. 323–330, Jul. 1996. doi: 10.1049/ip-epa:19960374.

[21] P. Li, Y. Wang, G. P. Adam, D. Holliday, and B. W. Williams, "Three-phase AC–AC hexagonal chopper system with heterodyne modulation for power flow control enhancement," *IEEE Trans. Power Electron.*, vol. 30, no. 10, pp. 5508–5521, Oct. 2015. doi: 10.1109/TPEL.2014.2378018.

[22] F. Zhang, X. Fang, F. Z. Peng, and Z. Qian, "A new three-phase AC–AC Z-source converter," in *Proc. IEEE APEC*, Dallas, TX, USA, Mar. 2006, pp. 19–23.

[23] S. A. Deraz, H. Z. Azazi, M. S. Zaky, M. K. Metwaly, and M. E. Dessouki, "Performance investigation of three-phase three-switch direct PWM AC/AC voltage converters," *IEEE Access*, vol. 7, pp. 11485–11501, 2019. doi: 10.1109/ACCESS.2019.2892523.

[24] J. Thankachan and S. George, "A novel switching scheme for Three phase PWM AC Chopper fed induction motor," in *Proc. IEEE IICPE*, Delhi, India, Dec. 2012, pp. 1–4.

[25] V. Thanyaphirak, V. Kinnares, and A. Kunakorn, "Soft starting control scheme for three-phase induction motor fed by PWM AC chopper," In *Proc. IEEE ICEMS*, Hangzhou, China, Oct. 2014, pp. 92–95.

[26] S. A. Deraz and H. Z. Azazi, "Current limiting soft starter for three phase induction motor drive system using PWM AC chopper," *IET Power Electron.*, vol. 10, no. 11, pp. 1298–1306, Sep. 2017. doi: 10.1049/iet-pel.2016.0762.

[27] A. Ukil, R. Bloch, and A. Andenna, "Estimation of induction motor operating power factor from measured current and manufacturer data," *IEEE Trans. Energy Convers.*, vol. 26, no. 2, pp. 699–706, Jun. 2011.

[28] A. M. A. Amin, "Power factor improvement of AC chopper-based induction motor drive," in *Proc. IEEE IECON*, San Jose, CA, USA, Nov./Dec. 1999, pp. 915–920.

[29] M. Kale, M. Karabacak, and B. Saracoglu, "A novel hysteresis band current controller scheme for three phase AC chopper," *Int. J. Elect. Power Energy Syst.*, vol. 44, no. 1, pp. 219–226, Jan. 2013. doi: 10.1016/j.ijepes.2012.07.013.

[30] H. Z. Azazi, S. M. Ahmed, and A. E. Lashine, "Single-stage three-phase boost power factor correction circuit for AC–DC converter," *Int. J. Electron.*, vol. 105, no. 1, pp. 30–41, Jan. 2018. doi: 10.1080/00207217.2017.1335800.

[31] M. K. Metwaly, H. Z. Azazi, M. S. Zaky, and S. A. Deraz, "Power factor correction of four-switch three-phase inverter-fed sensorless induction motor drives with partial electrical free measurement," *Electric Power Compon. Syst.*, vol. 46, no. 7, pp. 837–851, 2018. doi: 10.1080/15325008.2018.1509912.

[32] P. A. Dahono, D. Amirudin, A. Rizqiawan, and D. Deni, "Analysis of input and output ripples of PWM AC choppers," *ITB J. Eng. Sci.*, vol. 40, no. 2, pp. 91–109, Nov. 2008. doi: 10.5614/itbj.eng.sci.2008.40.2.2.

**MOHAMED K. METWALY** received the B.Sc. (Hons.) and M.Sc. degrees in electrical engineering from Menoufia University, Shibin El-Kom, Egypt, in 1999 and 2003, respectively, and the Ph.D. degree (Hons.) in electrical engineering from the Vienna University of Technology, Vienna, Austria, in 2009. In 2000, he joined the Department of Electrical Engineering, Faculty of Engineering, Menoufia University, as an Instructor, where he became an Assistant Lecturer, in 2003. From 2010 to 2015, he was a Lecturer with the Department of Electrical Engineering, Faculty of Engineering, Menoufia University, where he became an Assistant Professor, in 2015. He joined the Department of Electrical Engineering, Faculty of Engineering, Taif University, Saudi Arabia. His research interests include control of ac machines, applications of power electronics, power factor correction converters, sensorless control of electric drives, renewable energy applications, stability analysis of control systems, observers and estimators, and digital signals processing-based real-time control.

**HAITHAM Z. AZAZI** was born in Sharkia, Egypt, in 1979. He received the B.Sc., M.Sc., and Ph.D. degrees in electrical engineering from Menoufia University, Shibin El-Kom, Egypt, in 2003, 2008, and 2011, respectively. He joined the Department of Electrical Engineering, College of Engineering, King Khalid University, Saudi Arabia. Since 2016, he has been an Assistant Professor with the Department of Electrical Engineering, Faculty of Engineering, Menoufia University. His research interests include applications of power electronics, power factor correction converters, LED lighting systems, renewable energy applications, control of electrical machines, and DSP-based real-time control.

**SAID A. DERAZ** was born in Menoufia, Egypt, in 1976. He received the B.Sc., M.Sc., and Ph.D. degrees in electrical engineering from Menoufia University, Shibin El-Kom, Egypt, in 1999, 2004, and 2008, respectively. He joined the Department of Electrical Engineering, King Abdulaziz University, Rabigh. He has been a Lecturer with the Department of Electrical Engineering, Faculty of Engineering, Menoufia University, since 2008. His current research interests include applications of power electronics, power quality, control of electrical machines, power factor correction converters, sensorless control of electric drives, stability analysis of control systems, DSP-based real-time control, and renewable energy systems.

**MOHAMED E. DESSOUKI** was born in Bohiera, Egypt, in 1976. He received the B.Sc., M.Sc., and Ph.D. degrees in electrical engineering from the Faculty of Engineering, Suez Canal University, in 1999, 2004, and 2010, respectively. In 2000, he joined the Department of Electrical Engineering, Faculty of Engineering, Suez Canal University, as a Demonstrator. Then, he became an Assistant Lecturer, from 2004 to 2010, and has been a Lecturer, since 2010. He joined the Department of Electrical Engineering, King Abdulaziz University, Rabigh. His main professional interests include ac and dc drives, direct torque and field-oriented control techniques, and DSP control and power electronics applications.

**MOHAMED S. ZAKY** was born in Menoufia, Egypt, in 1978. He received the B.Sc., M.Sc., and Ph.D. degrees in electrical engineering from Menoufia University, Shibin El-Kom, Egypt, in 2001, 2005, and 2008, respectively. In 2002, he joined Menoufia University as an Instructor, where he became an Assistant Lecturer, in 2006. From 2008 to 2013, he was a Lecturer with the Department of Electrical Engineering, Faculty of Engineering, Menoufia University, where he was an Assistant Professor, from 2013 to 2018. In 2018, he was promoted with Scientific Excellence to a Professor in the field of automatic control with the Department of Electrical Engineering, Faculty of Engineering, Menoufia University. He joined the Department of Electrical Engineering, Northern Border University, Arar, Saudi Arabia. His research interests include control of electrical machines, stability analysis of control systems, observers and estimators, applications of power electronics, DSP-based real-time control, and sensorless control of electrical drives.

● ● ●